

Towards understanding phosphorus distribution in coal: A case study from the Bowen Basin

Brooke Davis*
The University of Queensland
St Lucia, QLD, 4069
b.davis2@uq.edu.au

Sandra Rodrigues
The University of Queensland
St Lucia, QLD, 4069
s.rodrigues@uq.edu.au

Joan Esterle
The University of Queensland
St Lucia, QLD, 4069
j.esterle@uq.edu.au

*presenting author

SUMMARY

In coal, phosphorus can occur in a variety of minerals but apatite $\text{Ca}_5(\text{PO}_4)_3(\text{OH}, \text{F}, \text{Cl})$ is the most common. This mineral is often observed within the cell-lumens (<20 microns) of inertinite macerals, although fracture-infilling apatite has been reported. Its size and main occurrence within the cell lumens makes it difficult to liberate the apatite by current coal beneficiation strategies. It also reduces porosity and clogs flow paths for gas drainage. Present-day mineral distributions reflect the origins and geological history of the coal and fluids moving through it. Therefore, understanding the geological controls of these distributions within the coal seams can help in prediction and developing mitigation strategies.

Interrogation of spatial litho- and bulk chemical-data sets within Permian coals at a single deposit affected by igneous intrusions, faults and seam splits was undertaken. Preliminary results in the study-area show elevated phosphorus contents are common in the roof and floor of the parent coal seam. However, these elevated contents transgress lithotypes, up-dip along the flanks of an anticline that is also proximal to a fault, a dyke and a rider seam split. The findings from this work provided the framework for samples selection for detailed microanalysis.

Initial electron probe results show multiple phosphate minerals including: apatite and crandallite $[\text{CaAl}_3(\text{PO}_4)(\text{PO}_3\text{OH})\text{OH}_6]$. There are at least two mode of occurrence of the apatite minerals: cell-lumen- and fracture-infilling, with the former most common. The cell-infilling apatite is thought to reflect either syngenetic or epigenetic mineralisation; while the fracture-infilling apatite formed later, post coalification. This is interpreted to have formed via fluids migrating through permeable and porous pathways created during geological deformation. Preliminary infrared spectroscopy results show the fracture-infilling apatite is relatively crystalline and lacking a hydroxyl peak which could reflect fluoridation. Preliminary cathodoluminescence data show this fracture-infilling apatite, as well as those in the pores, appears to be an epigenetic mineral phase that potentially formed from a single-phase fluid.

The spatial distribution of bulk chemical data suggests a spatial dependence between elevated phosphorus contents and post- or syn-depositional features. However, a conclusive relationship between mode of occurrence, apatite chemistry and proximity to depositional and post-depositional features has not yet been found. Therefore, alternative analytical methods to discriminate between phosphorus-bearing minerals formed from such processes are proposed.

Key words: Phosphorus, Coal, Permian, Apatite, Fluorine.

INTRODUCTION

Phosphorus in either coal-derived coke or iron ore is an undesirable trace element during steel making. This is because elevated phosphorus contents within the smelter can affect the ductility of the subsequent steel. Therefore, restrictions are commonplace, imposed to mitigate deleterious elements such as phosphorus. Current density beneficiation does not always reduce phosphorus contents from product coal to meet the imposed tolerances. This is because phosphorus can occur as small (<20 μ), discrete inorganic minerals within the coal particles as described by Ward (2016) and so can occur across different size fractions and densities (Partridge *et al.*, 1992). A number of mine sites have observed a concentration of phosphorus contents within their product coals.

This paper describes the occurrence and distribution of phosphorus bulk chemistry and phosphorus-bearing minerals within Late Permian coal seams on the north-eastern flank of the Bowen Basin. A systematic analysis of deposit-scale data was used to refine the approach taken for the sampling and micro-analysis. If the origins of the phosphorus-bearing minerals can be understood, then their distribution might be predicted and lead to improved blending, scheduling, and mitigation strategies.

Many mechanisms have been identified as influencing the origin of mineral matter within coal. These include: source-rock, marine influences, hydrothermal fluids, groundwater and volcanic ash (Dai *et al.*, 2012). The mineral matter may form external to the peat swamp and be washed or blown in (detrital) and it may also form in place (authigenic). Authigenic minerals may form early, during peat accumulation (syngenetic), or during rank advance or post-coalification (epigenetic) (Ward, 2016).

The precipitation and dissolution of inorganic minerals such as phosphate minerals are determined by specific environmental conditions, including: ion availability, pH and redox potential (Dai *et al.*, 2015). Apatite, $\text{Ca}_5(\text{PO}_4)_3(\text{F}, \text{Cl}, \text{OH})$, is stable under neutral to alkaline conditions; meanwhile aluminophosphates such as the goyazite-crandallite series, $\text{SrAl}_3(\text{PO}_4)_2(\text{OH})_5$ to $\text{CaAl}_3(\text{PO}_4)(\text{PO}_3\text{OH})\text{OH}_6$, exhibit reduced solubility under acidic conditions (Dai *et al.*, 2015).

In coal, apatite is the main phosphate mineral observed. The apatite identified by electron probe analysis can be seen infilling both the cell-lumens of inertinite macerals and the surface of cleats and/or fractures (Ward *et al.*, 1996, Ward, 2016). The cell-infilling phases are interpreted as having formed early during peat accumulation, with some authors such as Ward (2016) suggesting the phosphorus derived from decaying plant matter or fluid-rock interactions at the peat bed surface. Another source of the phosphorus could be weathered granites and felsic volcanic rocks as proposed by Salimen (2006) and Sevastjanova *et al.* (2012). The fracture-infilling phase is thought to have formed late, post-coalification, subsequent to the conditions required to form the cleat/fracture (Davis *et al.*, 2006, Permana *et al.*, 2013).

The study area is within the Permo-Triassic Bowen Basin as shown in Figure 1. It extends from Collinsville in Central Queensland to northern NSW, where it connects to the Gunnedah and Sydney basins.

The Bowen Basin consists of a 10 km sequence of shallow-marine to terrestrial clastic sedimentary rock, including coking and thermal coal product reserves (Fielding *et al.*, 1993). The primary resources include Late Permian Rangal and Moranbah Coal Measures and their lateral equivalents, as shown in Figure 2.

The Bowen Basin tectonic history is a series of complex subsidence, closure and uplift events that occurred over 200 Ma (Totterdell *et al.*, 2009). Considering this, it is possible that several geological processes contributed to the current *in situ* phosphorus distribution within the coal seams and adjacent strata. For instance, faulting is common within the coal measures throughout the basin with structural complexity increasing within the Nebo Synclinorium towards the north-east (Korsch and Totterdell, 2009). The central, western and southern areas are mildly deformed, with no major faulting observed throughout the study-area (Korsch *et al.*, 2009). Igneous intrusions significantly increase within the northern Bowen Basin (Hamilton, 1985). They range in age from Early Cretaceous (gabbroic to granodiorite intrusions) to Cenozoic (basaltic to rhyolitic extrusive rocks) (Hamilton, 1985). It is believed the emplacement of igneous intrusions has resulted in local contact metamorphism including variations in coal rank and mineralogy (Schimmelmann *et al.*, 2009).

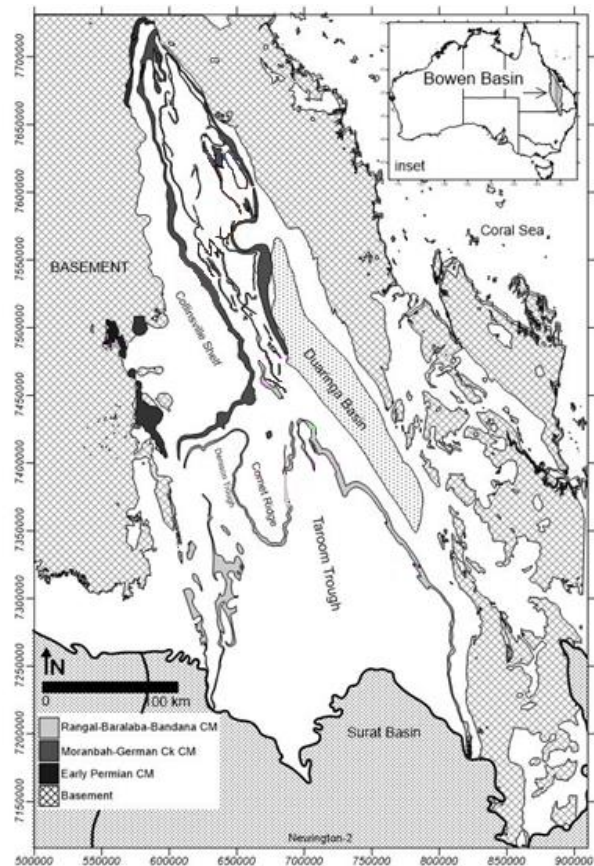


Figure 1 Structural elements and coal measures of the Bowen Basin.

Age	Southern Area			Northern Area	Group
	Denison Trough	Comet Ridge and Northern Taroom Trough	Northeastern Taroom Trough	Collinsville Shelf and Nebo Synclinorium	
Upper Permian	Bandana Formation	Rangal Coal Measures	Baralaba Coal Measures	Rangal Coal Measures	Blackwater Group
	Burngrove Formation	Burngrove Formation	Kaloola Member	Burngrove Formation	
	Black Alley Shale		Gyranda Formation	Middle Main Seams	
	Peawaddy Formation	Fair Hill Formation		Fair Hill Formation	
		MacMillan Formation	Flat Top Formation	Moranbah Coal Measures	
	Catherine Sandstone	German Creek Formation			

Figure 2 Sequence stratigraphy of the Bowen Basin (Avaz et al., 2015) (modified after Anderson (1985)).

SAMPLING AND ANALYTICAL TECHNIQUES

Data and samples were analysed for a single seam across a single deposit within the Rangal Coal Measures, northern Bowen Basin. The seam is gently folded and exhibits splitting, is faulted and intruded. Samples were collected proximal and distal to these geological features to determine whether they influenced the conditions conducive to apatite precipitation.

Samples were obtained from the mine site. During drilling, the coal seam was logged for lithotype distribution, and sampled on 50 cm contiguous intervals. Samples were crushed and floated at 1.6g/cc, split and analysed for P₂O₅ (%) in ash following AS 1038.9.1-2000 from which phosphorus (%) was calculated.

Phosphorus contents were plotted down-hole in SKUA-GOCAD™ with respect to the seam geometry, to look for spatial patterns that could allude to the origins of the phosphorus. Subsequently, selected samples were potted in resin and polished for microscopic analysis using scanning electron microscopy with energy dispersive x-ray spectrometry (SEM-EDS). Sub-samples were further analysed using infrared spectroscopy and cathodoluminescence techniques.

RESULTS

Across the mine site the coal seams dip to the west. The seams are gently folded with the axes striking east-west and are commonly displaced by minor (2m to 10m throw) normal faults as shown in Figure 3. These seams are intruded by a dyke swarm, which is more prominent in the northern-end of the deposit. A cross-section shows the seams coalescing in the centre. This coalesced seam splits both to the northern- and southern-ends of the deposit, forming a crab-like structure. The coalesced seam folds and forms into a syncline in the north and an anticline in the centre (as shown in Figure 3), with the axes striking east. The phosphorus contents are highly variable along strike, down dip and vertically within the coal seams across the deposit. In the syncline, the phosphorus contents are elevated in the roof and floor of the coalesced seam, while towards the south of the section, elevated phosphorus values appear to migrate from the floor towards the crest of the anticline.

There appears to be little to no correlation between P₂O₅ and coal composition, as phosphorus contents vary across a single coal lithotype as shown in Figure 4. Cross-correlations of oxide data (CaO, BaO, SrO and P₂O₅) are weakly correlated as shown in Figure 4. Therefore, the regression analysis could not be used discriminate phosphorus-bearing minerals, even when ply and geographic location domains were applied to the dataset. These poor correlations are most likely due to multiple sources for elements associated with phosphorus-bearing minerals, such as calcium, for which the source include: calcite, ankerite and apatite, as identified by SEM-EDS.

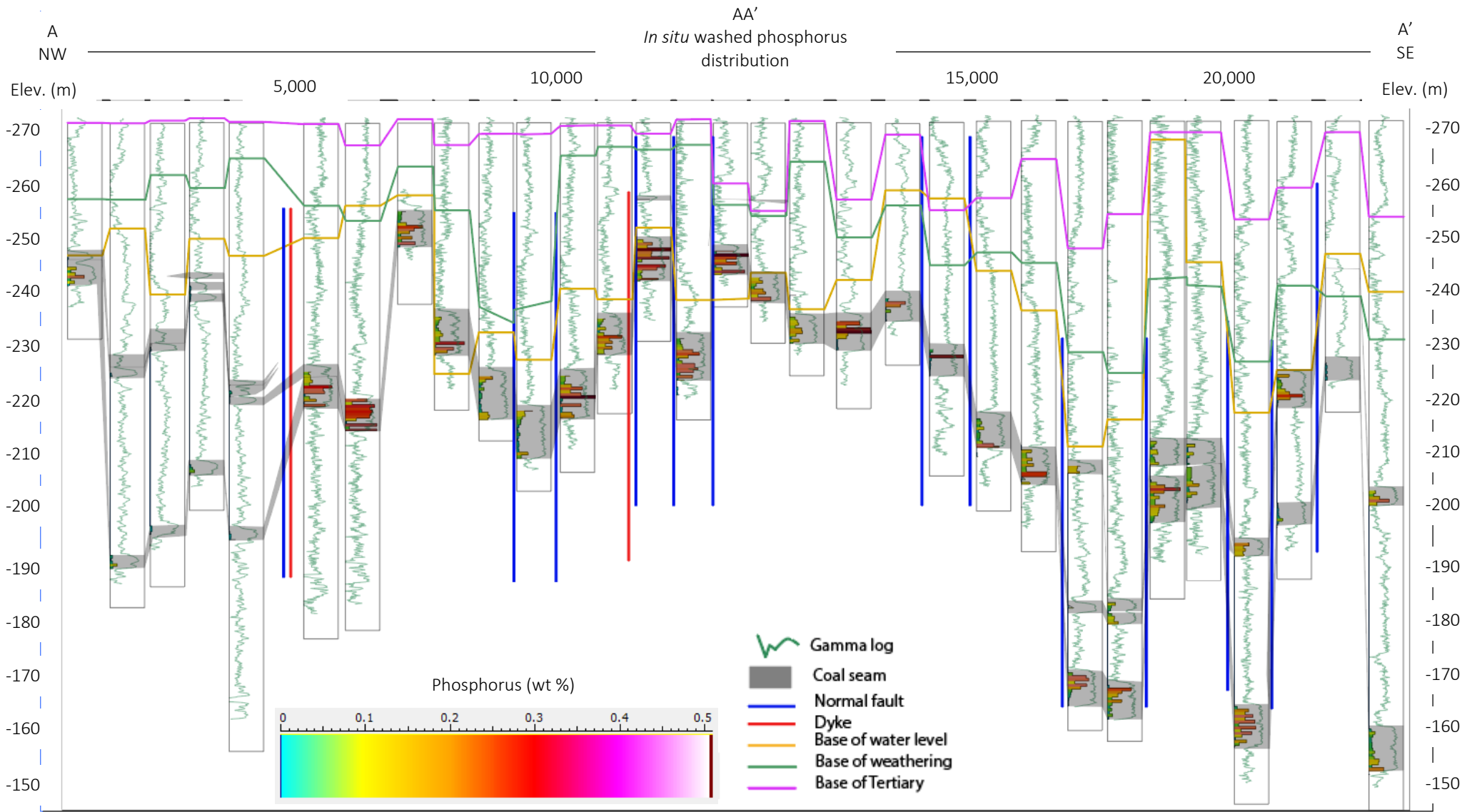


Figure 3 Cross-section flattened to topography of washed coal bulk phosphorus distribution within the coalesced seam and its splits.

Therefore, since the bulk litho- and chemical-data were insufficient in discriminating the phosphate minerals and finding a suitable predictor such as maceral assemblage, detailed micro-analysis was undertaken to determine the mode of occurrence of the phosphorus and to find indicators of geochemical conditions of precipitation.

SEM-EDS and reflected light microscopy results show that most of the mineral matter occurs as cell-infillings within the inertinite-group macerals. This is more common within the semifusinite and fusinite coal particles, as shown in Figure 5(a). The main mineral groups observed were carbonates and clays, being mainly calcite and kaolinite, respectively. The primary phosphorus-bearing mineral phase observed was the calcium-phosphate apatite with fluorine detected, which also occurred as cell-infillings. Alternative mineral occurrences have been observed, including calcite and apatite within fractures. For example, Figure 5(b) shows a fracture-infill apatite along the edge of a semifusinite maceral. From top to bottom of the seam there is little variation in the mode of occurrence of the phosphate minerals. The apatite occurs only as a minor mineral phase in the total inorganic mineral assemblage. Optically the apatite seems amorphous and typically occurs as an apparent overgrowth on kaolinite. Minor calcium-alumino phosphate, crandallite is also observed, associated within the same maceral grain as an apatite and kaolinite (Figure 5(a)). Some apatite grains were observed as monomineralic aggregates while others were polymineralic, sharing the space within the cell lumen of inertinite maceral with other inorganic phases such as kaolinite and chalcopyrite. Phosphorus bound to the organic carbon was not detected using this analytical approach.

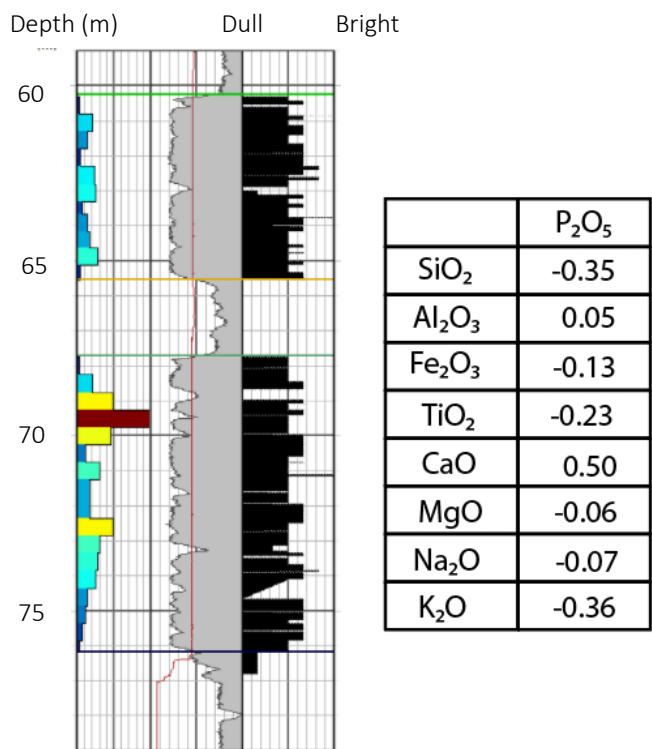


Figure 3 (a) Down-hole phosphorus (%) contents as analysed on the ash with logged coal characterization and (b) Regression analysis of elemental ash data.

Phosphorus bound to the organic carbon was not detected using this analytical approach.

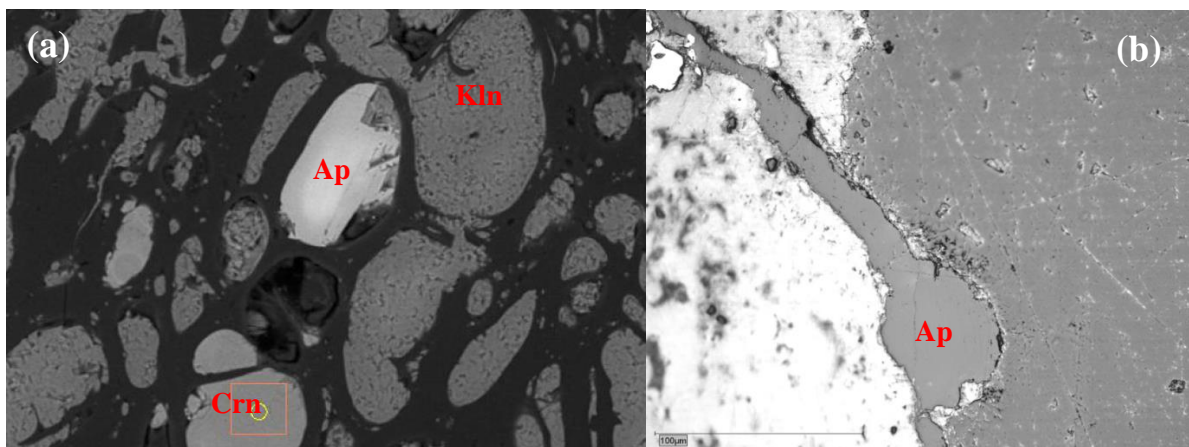


Figure 5 (a) SEM-EDS of fusinite maceral. Cell-infilling apatite (Ap), Kaolinite (Kln) and Crandallite (Crn) have been identified. (b) Reflected light microscopy of a fracture-infill apatite within a semi-fusinite.

Preliminary infrared spectroscopy analysis shown in Figure 6 illustrates the infrared spectroscopy spectra for the fracture-infilling apatite, which shows an absence of both a hydroxyl peak at ~3,600 cm⁻¹ and carbonate-structure at ~800 cm⁻¹. Note the spectra for the epoxy resin, a synthetic, pure hydroxyapatite and a pore-infilling apatite are given for comparison. This figure shows the fracture-infilling apatite spectra is more narrow and defined than the pore-infilling apatite from another location within the Bowen Basin but more broad than the synthetic hydroxyapatite. This suggests that the fracture-infilling apatite is more crystalline than the pore-infilling apatite but less crystalline than the synthetic hydroxyapatite.

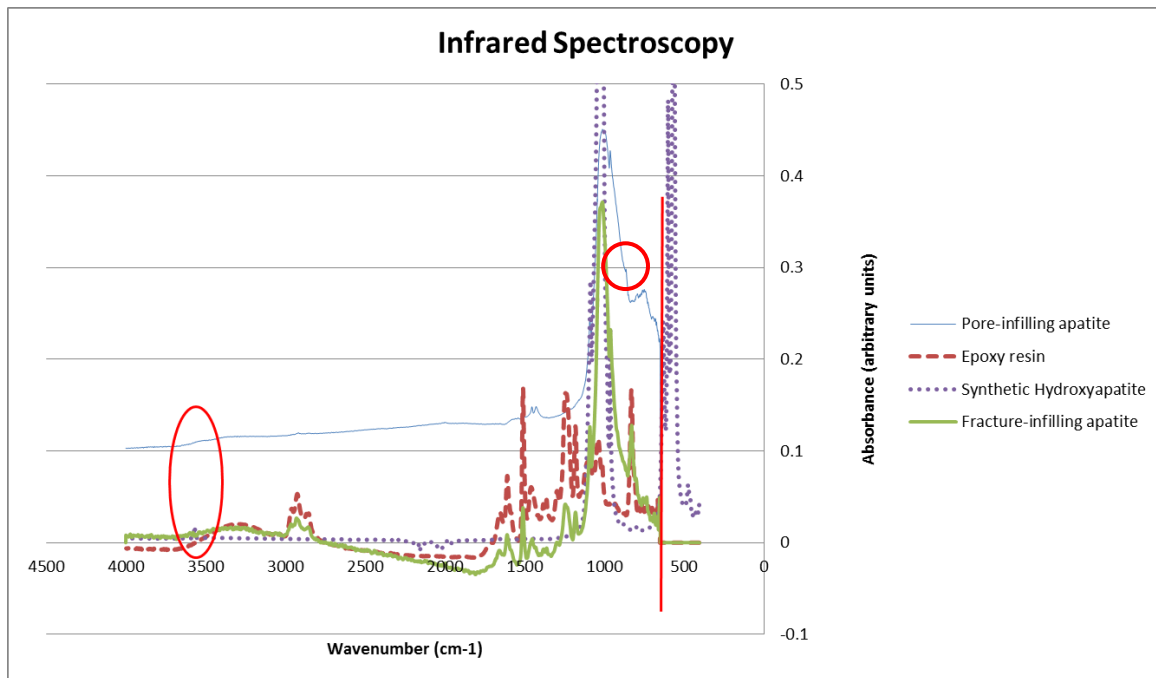


Figure 6 FTIR of different apatite grains (pore- and fracture-infilling and synthetic). The location of the hydroxyl-band at $3,600\text{ cm}^{-1}$ and the carbonate band at 800 cm^{-1} have been marked by the circles. The detector on the microscope is high sensitivity and liquid N₂ cooled to measure the very small IR signal you get in a microscope. For this study it was necessary to use the microscope to optically find the apatite grains, therefore it was not possible to extend the detection limit into the low wavenumber region (this cut-off is denoted by the vertical line). So, unfortunately signature phosphate peaks below 600 cm^{-1} were missed, but these grains were confirmed as apatite from the SEM-EDS analysis and did not affect the overall interpretation.

Preliminary relative X-ray intensity maps illustrated in Figure 7 shows phosphorus readily associated with the element fluorine. To date, fluorine has not been observed with alternative mineral phases. The apatite is relatively homogenous with no chemical (phosphorus and fluorine) or structural zonation observed within the apatite grains.

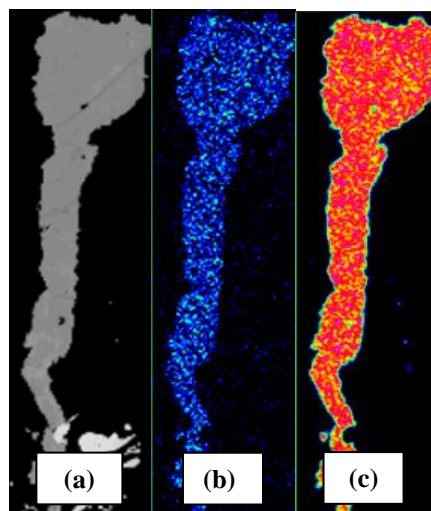


Figure 7 Fracture-infilling apatite (a) back-scattered electron (BSE) image, (b) F-K α X-ray map and (c) P-K α X-ray map

DISCUSSION AND CONCLUSIONS

Previous research suggests that phosphorus is derived either from the original plant matter or fluid-rock interactions at the peat-bed interface (Ward *et al.*, 1996). Upon decomposition, the phosphorus is released as H_2PO_4^- where the phosphorus is taken up by living plants or it complexes with available ions (Ward, 2016). This is often based on the phosphate minerals occurring within the cell-lumens of inertinite macerals and that coal seams typically have reduced permeability for fluid migration. Although similar observations have been made as part of this study, the spatial distribution shows elevated phosphorus contents progressively extending from the seam floor up to the seam roof which does not appear to support this ‘early’ model. This more extensive distribution of phosphorus contents occurs as the seam becomes intruded, faulted and has more complex seam geometry and, thus, suggesting a more

complicated history. This could either mean that there are multiple sources of phosphate minerals and controls and there is also potential remobilisation of early phosphates to later-stages by fluid migrations within the coal seams.

Emplacement of phosphate minerals could have been contemporaneous with subsidence and burial or formed post-coalification. For example, the influx of clastic material (forming a seam split) during deposition may have introduced more phosphorus into the peat environment. As the clastic load increased the pressure on the peat increased. This squeezed the phosphorus-rich waters out of the peat, and with a decrease in pressure migrated upwards, saturating the peat profile. Alternatively Esterle (1999) proposes that a redox change can occur at the sediment-load interface causing a “roll front”. This redox change increased microbial activity, releasing the phosphorus contained within sediments in the “roll front” (Esterle, 1999, Salimen, 2006). On the other hand, late-stage hydrothermal fluids could have migrated along permeable zones. Roof and floor contacts, faults and fractures could have acted as conduits to fluid flow, resulting in localized zones of phosphate mineralization (Davis *et al.*, 2006).

Regression analyses of P₂O₅ relative to other variables such as major oxides in coal ash, yielded few notable results. However, a mild correlation (50%) with CaO was observed. This together with the observations made using SEM-EDS illustrate there are multiple sources for both phosphorus and calcium such as crandallite and calcite, respectively. Apatite, kaolinite and crandallite have been observed within cell-lumens of a single inertinite maceral particle (Figure 5a). The apatite is optically amorphous with no chemical or morphological zonation observed within the individual grains. However, it appears that these occurrences are not spatially constrained by coal lithotype. Therefore, additional techniques such as infrared spectroscopy and cathodoluminescence are being undertaken to further characterize the phosphorus- and fluorine- elemental distributions to try to find some spatial variation.

Infrared spectroscopy results show that the fracture-infilling apatite is crystalline with no hydroxyl peak observed and a reasonably narrow, well-defined phosphate band. These results suggest that this grain is fluoridated, confirming the SEM-EDS results. However, this grain is less crystalline than the synthetic hydroxyapatite, contradicting previous research by Campillo *et al.* (2010) who showed, using a similar technique, that an increase in fluoridation of synthetic apatite grains were indicated by both a more narrow and defined phosphate vibrational band at approximately 960cm⁻¹. There is also a lack of carbonate-structure within the spectra; this could suggest there is little-to-no- carbonate within this particular apatite, potentially indicating that this apatite is not of biological origin. Because infrared spectroscopy can give compositional and structural changes in minerals such as apatite (Wopenka and Pasteris, 2005), this technique could be used to discern the degree of fluoridation of the apatite grains (Campillo *et al.*, 2010). Therefore, changes in fluorine substitution within the crystal structure could be observed between samples taken in active versus passive tectonic settings. This would be useful in identifying how substitution varies spatially and stratigraphically. Unfortunately this technique is qualitative and can therefore not quantify the relative elemental concentrations, therefore requiring additional analytical methods.

Preliminary relative X-ray intensity maps show that the phosphorus and fluorine strongly correlate and that the fracture-infilling apatite is relatively homogeneous. That is, no chemical zonation with respect to phosphorus or fluorine concentration has been observed within this particular grain. This could suggest that this apatite derived from a single fluid source (Zirner *et al.*, 2015). However, more work is required to ascertain the conditions under which these phosphate minerals precipitated, as well as the significance of these findings spatially.

In conclusion, bulk-phosphorus data suggests a relationship between *in situ* phosphorus distribution and geological features such as igneous intrusions, faulting and seam splitting. Microanalysis has successfully identified multiple phosphate-minerals. However, their distribution does not appear to be spatially dependent. Preliminary infrared spectroscopy results suggest that the fracture-infilling apatite is not biological in origin. It is also chemically homogeneous suggesting it precipitated from a single fluid phase. Although more work is still to be undertaken, the preliminary results show the potential in taking a micro-analytical approach for mineral discrimination in order to understand fluid source and potential controls on *in situ* spatial distribution.

FUTURE WORK

To try to constrain and fingerprint the fluid source, emplacement mechanisms and timing we recommend that further work be undertaken. This is to occur both laterally across and stratigraphically within the Bowen Basin rock and coal strata. For example, detailed microanalysis such as electron probe analysis could be conducted on samples from different geological domains (igneous intrusions, faulting or seam splitting). To do this, indicators of geochemical conditions of precipitation are being sought. This is because reflected-light and electron probe microscopy have proven insufficient in discriminating between texture changes, if they exist, between fracture- and cell-infilling apatite grains. Therefore, additional analytical techniques are being explored. These are being undertaken to find key features that may indicate source and timing of mineralization. These include: rare earth element chemistry via cathodoluminescence, electron probe micro-analysis (EPMA), fluorine concentration via EPMA and laser-induced breakdown spectroscopy (LIBS), crystallinity via infrared spectrometry and electron-backscatter diffraction, as well as Carbon (¹³C/¹²C) and oxygen (¹⁸O/¹⁶O) and strontium (⁸⁷Sr/⁸⁶Sr) stable isotopes.

ACKNOWLEDGMENTS

The authors of this paper wish to thank ACARP (Australian Coal Industry’s Research Program) for funding this project, as well as the coal industry for allowing the authors to use data and findings as part of this study, and for its support in allowing the presentation of this work. Relative X-Ray intensity maps were acquired by H. Cathey and IR spectra were acquired by L. Rintoul at the *Central Analytical Research Facility* operated by the *Institute of Future Environments (QUT)*.

REFERENCES

- Ayaz, S. A., Esterle, J. S. & Martin, M. A. 2015. Spatial variation in the stratigraphic architecture of the Fort Cooper and equivalent coal measures, Bowen Basin, Queensland. *Australian Journal of Earth Sciences*, 62, 547-562.
- Campillo, M., Lacharaise, P. D., Reparaz, J. S., Goñi, A. R. & Valiente, M. 2010. On the assessment of hydroxyapatite fluoridation by means of Raman scattering. *The Journal of Chemical Physics*, 132, 244501.
- Dai, S., Hower, J. C., Ward, C. R., Guo, W., Song, H., Amp, Apos, Keefe, J. M. K., Xie, P., Hood, M. M. & Yan, X. 2015. Elements and phosphorus minerals in the middle Jurassic inertinite-rich coals of the Muli Coalfield on the Tibetan Plateau. *International Journal of Coal Geology*, 144-145, 23-47.
- Dai, S., Ren, D., Chou, C.-L., Finkelman, R. B., Seredin, V. V. & Zhou, Y. 2012. Geochemistry of trace elements in Chinese coals: A review of abundances, genetic types, impacts on human health, and industrial utilization. *International Journal of Coal Geology*, 94, 3-21.
- Davis, B., Esterle, J. S. & Keilar, D. Determining the geological controls on the spatial distribution of phosphorus within coal seams mined at South Walker Creek Mine, Bowen Basin, Central Queensland, Australia. *Advances in the Study of the Sydney Basin*, 27-29 November 2006 2006 Woollongong, Australia. 28-35.
- Esterle, J. S. 1999. Controls on Phosphorus Variability at the Minescale. The 33rd Newcastle Symposium on Advances in the Study of the Sydney Basin, 1999 University of Newcastle, NSW. 193-199.
- Fielding, C. R., Falkner, A. J. & Scott, S. G. 1993. Fluvial response to foreland basin overfilling the Late Permian Rangal Coal Measures in the Bowen Basin, Queensland, Australia. *Sedimentary Geology*, 85, 475-497.
- Hamilton, L. H. 1985. Igneous intrusions in the Bowen Basin.
- Korsch, R. J. & Totterdell, J. M. 2009. Subsidence history and basin phases of the Bowen, Gunnedah and Surat Basins, eastern Australia. *Australian Journal of Earth Sciences*, 56, 335-353.
- Korsch, R. J., Totterdell, J. M., Cathro, D. L. & Nicoll, M. G. 2009. Early Permian East Australian Rift System. *Australian Journal of Earth Sciences*, 56, 381-400.
- Partridge, A. C., J.D., S., Corcoran, J. F., Ward, C. R., Membury, W. B. & Lockhart, N. C. 1992. Phosphorus reduction in coal preparation -- a feasibility study. *Proceedings, 5th Australian Coal Science Conference*. Melbourne.
- Permana, A. K., Ward, C. R., Li, Z. & Gurba, L. W. 2013. Distribution and origin of minerals in high-rank coals of the South Walker Creek area, Bowen Basin, Australia. *International Journal of Coal Geology*, 116-117, 185-207.
- Salinen, R. 2006. *Geochemical Atlas of Europe. Part 1, Background information, methodology and maps*, Finland, Geological Survey of Finland.
- Schimmelmann, A., Mastalerz, M., Gao, L., Sauer, P. E. & Topalov, K. 2009. Dike intrusions into bituminous coal, Illinois Basin: H, C, N, O isotopic responses to rapid and brief heating. *Geochimica et Cosmochimica Acta*, 73, 6264-6281.
- Sevastjanova, I., Hall, R. & Alderton, D. 2012. A detrital heavy mineral viewpoint on sediment provenance and tropical weathering in SE Asia. *Sedimentary Geology*, 280, 179-194.
- Totterdell, J. M., Moloney, J., Korsch, R. J. & Krassay, A. A. 2009. Sequence stratigraphy of the Bowen-Gunnedah and Surat Basins in New South Wales. *Australian Journal of Earth Sciences*, 56, 433-459.
- Ward, C. R. 2016. Analysis, origin and significance of mineral matter in coal: An updated review. *International Journal of Coal Geology*, 165, 1-27.
- Ward, C. R., Corcoran, J. F., Saxby, J. D. & Read, H. W. 1996. Occurrence of phosphorus minerals in Australian coal seams. *International Journal of Coal Geology*, 30, 185-210.
- Wopenka, B. & Pasteris, J. D. 2005. A mineralogical perspective on the apatite in bone. *Materials Science and Engineering: C*, 25, 131-143.
- Zirner, A. L. K., Marks, M. a. W., Wenzel, T., Jacob, D. E. & Markl, G. 2015. Rare earth elements in apatite as a monitor of magmatic and metasomatic processes: The Ilimaussaq complex, South Greenland. *LITHOS*, 228-229, 12-22.
- Ayaz, S. A., Esterle, J. S. & Martin, M. A. 2015. Spatial variation in the stratigraphic architecture of the Fort Cooper and equivalent coal measures, Bowen Basin, Queensland. *Australian Journal of Earth Sciences*, 62, 547-562.